Morphological Evolution and Intermetallic Behavior of Developed Scaffolds with Hydroxyapatite and Polylactic Acid for Bone Tissue Applications

E. C. Makinde[1], D. O. Daramola[1*] and O. S. I. Fayomi[2, 3*]

[1]*Department of Biomedical Engineering, Bells University of Technology, Ota, Ogun State, Nigeria*
[2]*Department of Mechanical Engineering, Bells University of Technology, Ota, Ogun State, Nigeria*
[3]*Faculty of Engineering and Built Environment, University of Johannesburg, Johannesburg, South Africa*

Corresponding authors: dodaramola@bellsuniversity.edu.ng, osfayomi@bellsuniversity.edu.ng

Received 08/12/2023; accepted 18/04/2024
https://doi.org/10.4152/pea.2026440102

Abstract

Patients with fractures require internal fixations, since treatment options are limited to metallic implants and autologous bone grafts. These limitations include chances of infection transference, quantity restrictions and the need for additional surgery. Bone tissue engineering seeks to address these limitations through the development of biocompatible bone scaffolds. This study fabricated a PLA based scaffold that sought to address some of the challenges associated with currently available treatment options. The methodology involved acquiring raw eggshells, which were rinsed with water and calcined with concentrated H_3PO_4. Hitherto, HAp powder was extracted from eggshells, and its presence was confirmed using color test. PLA (60,000 molecular weight) was procured from Sigma Aldrich, which was used with HAp powder, to form the composite, employing sol gel technique. SEM morphology established PLA, which has polymeric binding properties, as the 3D scaffold with the highest Ct (PLA/HAp (45/55 wt.%). It had a more consistent crystal and pore formation and weaker grain boundaries. FTIR analysis showed PLA characterizing peaks, and that functional groups present in 3D scaffold are not toxic to the body. X-RD spectra confirmed PLA and HAp presence in 3D scaffolds. However, peaks intensities decreased with lower Ct of HAp, and those of PLA increased in the 3D scaffold. This indicates that PLA and HAp particles have semi-crystalline and crystalline structures, respectively. Thus, 3D scaffolds can be tailored for many biomedical applications.

Keywords: bone fillers; characterizations; HAp; PLA; scaffold.

Introduction•

In today's world, cases of bone fracture are discovered yearly. For patients requiring internal fixations, i.e., bone fillers, the only viable options in developing nations are the

• The abbreviations list is in page 24.

use of metallic implants or autologous bone grafts, due to the lack of tissue engineering research and development. Although these metallic implants may be biocompatible, they are limited by the inability to hasten the bone healing process [1], and by their non-biodegradation, which often causes stress shielding. A solution for it is the fabrication of biocompatible scaffolds with adequate biodegradation rate [2]. A biodegradable scaffold means that there is a load balance between healing bone and degrading scaffold [3], which can be achieved through bone tissue engineering.

Extensive use of autologous bone grafts has been reported by research [4]. They can help in the treatment of people suffering from other bone diseases, defects and fractures such as osteonecrosis, spinal fusion, infections and birth abnormalities. While biological sources, especially autografts, are considered the standard criterion for bone-grafting materials, there are issues associated with their use. Autografts require an additional surgery, and they have quantity issues. Allografts bypass the problems linked with additional surgery and quantity restrictions, but there are also issues associated with reduced osteoinductive properties, immunogenicity and chances of infection transference [5]. For these reasons, biological bone-graft substitutes are being developed through bone tissue engineering. They comprise of scaffolds assembled from synthetic or natural biomaterials, and encourage cells migration, proliferation and differentiation [6]. Bone tissue engineering is an advancing field that seeks to overcome limitations of conventional treatments for bone diseases and defects. It aims to produce new functioning tissues that adapt to the host with no adverse reactions [7]. This is considered a better approach to the treatment of bone diseases and defects, because the patient's tissue may undergo repair activity, once bone regeneration is completed [8].

Treatment options for bone diseases and defects are complex. For example, patients requiring bone fillers have to choose between metallic implants and autografts [1]. This shows that there is the need for further research on biological substitute bone grafts and scaffolds. It is important to ensure that bone scaffolds can be fabricated via scaffold fabrication methods and materials readily available in developing countries.

The present study aimed to fabricate and characterize a PLA-HAp scaffold bone tissue and surface, using sol-gel method, FTIR, SEM and X-RD techniques.

Experimental methods

Extraction of HAp from eggshells

In the extraction process of HAp from eggshells, several materials were used, such as raw eggshells, distilled water, deionized water, concentrated H_3PO_4, hot plate, oven, muffle furnace, magnetic stirrer, pH meter, mortar, pestle, crucibles, beakers, funnel, conical flask, stirrer, pipette and funnel paper. To perfect the process, eggshells were boiled in water for 30 min, using a hot plate. They were later dried in the oven, at 105 ºC, for 3h, and grounded. After 4 h in the oven, the dried eggshells were weighed, and then calcined at 800 ºC. Ignition loss on the calcined sample was assessed, to confirm CO_2 release. This was calculated by:

$$\frac{i-f}{f} \times 100\% \qquad (1)$$

where i and f are initial and final weight of the sample before and after calcination, respectively.

72.56 g calcined eggshells were then diluted in 994 mL distilled water. Concentrated H_3PO_4 was drop wise added, at a precise rate, to decrease the solution's pH to 8.5, which was kept at room temperature, for 24 h. Then, it was agitated for 30 min, with a magnetic stirrer, and left for another 24 h, at room temperature. The precipitate was filtered, carefully washed with deionized water and refiltered. The filtrate was oven-dried for 3 h, at 105 ºC, and then calcined at 800 ºC, for 6 h. The chemical reaction for calcination is:

$$CaCo_3 \xrightarrow{\Delta} CaO + CO_2 \qquad (2)$$

where Δ is the heat of reaction. The ignition loss was calculated using Eq. (3).

$$\text{Ignition loss} = \frac{103.45-72.56}{72.56} \times 100\% = 42.57\% \qquad (3)$$

CO_2 made up 44% $CaCO_3$. Ignition loss value of 42.57% shows there was 96.75% CO_2 release during calcination.

Fabrication of PLA-HAp bone scaffold using sol-gel technique

PLA with 60,000 molecular weight, purchased from Sigma-Aldrich (BCCG7787, USA), served as gel. HAp powder was extracted from eggshells, as shown in Fig. 1.

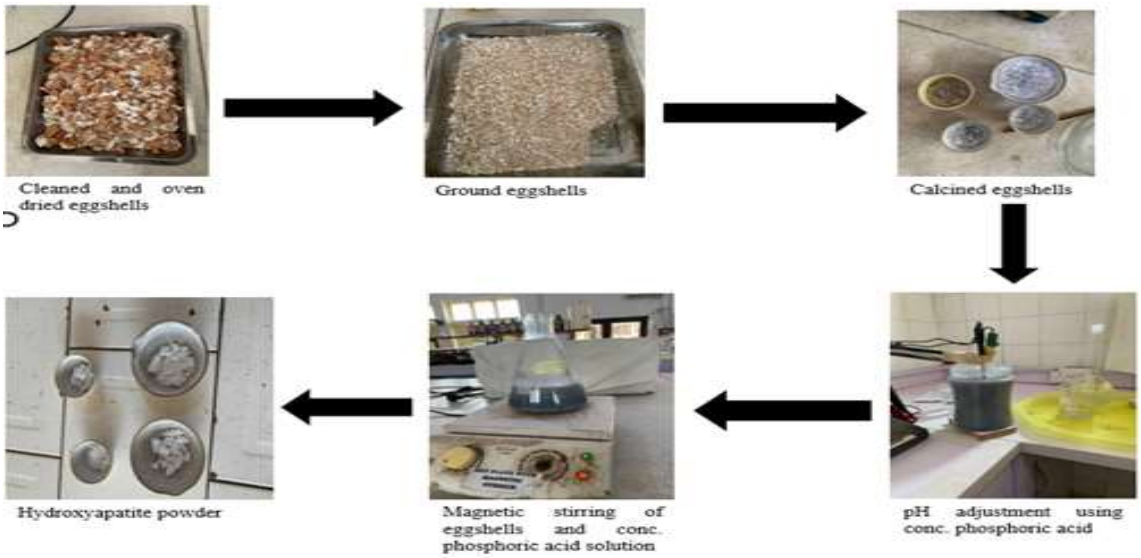

Figure 1: Extraction of HAp powder from eggshells.

Other materials were used, such as chloroform, rock salt, sonicator, weighing balance, mortar, pestle, sieve, mold, measuring cylinder, beakers and stirrer. HAp powder was grounded into a fine powder, and then sieved, using a 90-micrometer sieve. Then, a measured Ct (Table 1) of ground HAp powder was diluted in chloroform, using a sonicator, until a colloidal solution was formed.

Table 1: PLA/HAp ratio and weight table.

Sample composition	PLA ratio	Hap ratio	PLA weight	HAp weight
1- C1	15	85	0.15 g	0.85 g
2- C2	45	55	0.45 g	0.55 g

This process was done for PLA, until it was completely dissolved in chloroform. Then, PLA was mixed using a sonicator, until a colloidal solution was formed, to which rock salt (used as porogen), ranging from 0.5 to 1.5 mm, was added, after being homogeneously mixed. The solution was then poured into a mold, and left at room temperature, for the solvent to evaporate. The resulting scaffold was rinsed with deionized water, to allow for the rock salt dissolution. Fabricated 3D scaffolds arranged in the sample number order from the left are shown in Fig. 2.

Figure 2: Fabricated 3D scaffolds.

Characterization of PLA-HAp 3d scaffold

The microstructure response of the samples was determined using field emission SEM GEMINI Ultra 55. The samples were fixed on carbon tape and kept overnight, for drying. Then, they were gold-coated (100 nm) and examined under SEM, operated at 3 kV. The sol-gelled samples' chemical composition was analyzed by a FTIR spectrophotometer (Perkin-Elmer Spectrum one model), in attenuated total reflectance mode, from 4000 to 650 cm^{-1}, to determine the various functional groups present in the specimens. X-RD of the powdered composite samples was determined by Rigaku SmartLab diffractometer, operated at 40 kV and 40 mA, using Cu-Kα radiation. Data were collected and analyzed by Origin Pro software.

Results and discussion

Structural evaluation of developed PLA/HAP system

Figs. 3 and 4 clearly show the formation of crystals from the mixture of PLA and Hap, in C1 and C2.

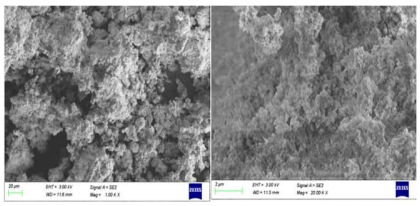

Figure 3: SEM of C1 at 1.00 and 20.00 K X magnification, respectively

From SEM results, it can be deduced that C2 (Fig. 4) has consistent crystal formation, with a compact, refined and well-oriented porous structure [9, 10].

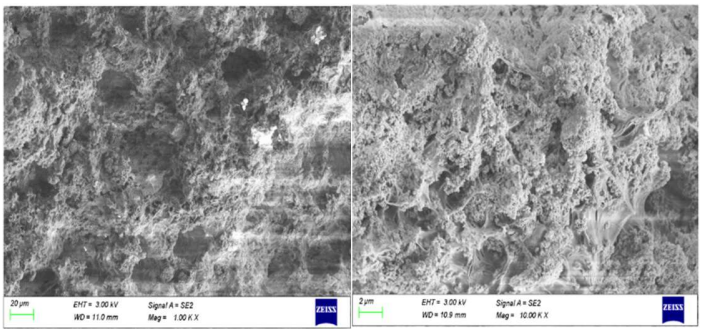

Figure 4: SEM of C2 at 1.00 and 20.00 K X magnification, respectively.

Although there are imperfections in the fabricated scaffold, such as white patches, at 1.00 and 2.00 K X magnifications, C2 has greater mechanical strength than that of C1, which is evident by weaker grain boundaries and more consistent crystal formation. Furthermore, a noticeable reason for improvement might be due to the refined flake's structure and Ct of PLA in the scaffolds, which was higher for C2 (0.45 g) than that of C1 (0.15 g). So, it can be assumed that PLA acted as polymeric binding agent within the samples.

Adsorption bonds effects on developed PLA/HAP materials

Figs. 5 and 6 show FTIR transition for C1 and C2, respectively.

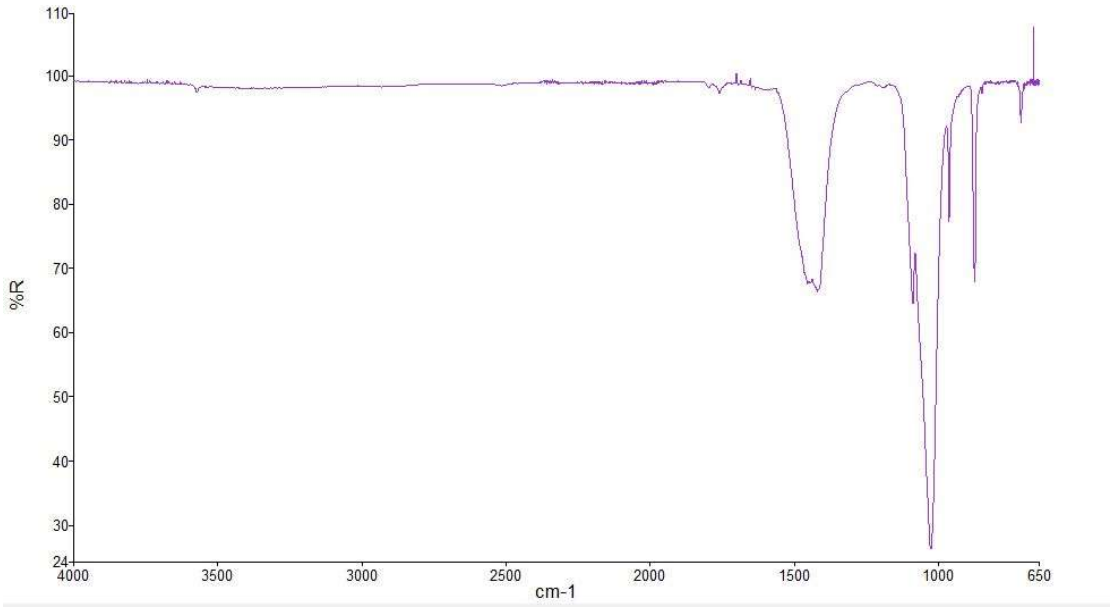

Figure 5: FTIR result of C1.

The developed scaffolds under investigation show five peaks' intensities. This is an indication of non-simple chemical activities. FTIR result shows the presence of peaks in the single bond area from 2500 to 4000 cm^{-1}. The broad absorption band in this area confirms the presence of hydrogen bonds in the scaffolds. The small sharp peak at 3571 (Fig. 5) and 3568 cm^{-1} (Fig. 6) attests for the existence of N-H stretching in the scaffolds. This indicates the presence of a primary amine bond.

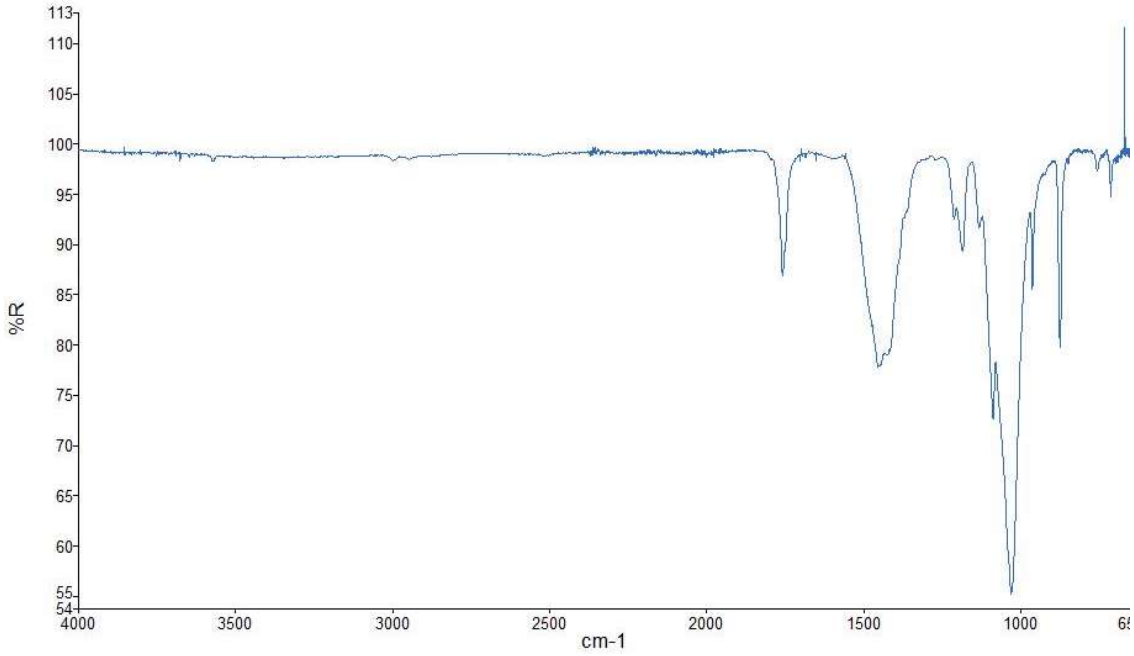

Figure 6: FTIR result of C2.

No peaks were seen from 3000 to 3200 cm^{-1}, which indicates that there is no aromatic structure in this region. There were no peaks detected in the triple bond area (2000-2500 cm^{-1}). However, peaks were detected in the double bond region (1500-2000 cm^{-1}). Peaks at 1740 (Fig. 5) and 1756 cm^{-1} (Fig. 6) confirm the presence of C=O chemical bonding, which indicates that there are esters in the scaffolds. The strong intensity from 1600 to 1650 cm^{-1} attests for the presence of double bonds in the scaffolds. Peaks at 1450 and 1454 cm^{-1} prove the existence of C-H bending within the scaffolds. Interestingly, there are methyl groups in the scaffold, which is in agreement with PLA's chemical properties of [11]. Identified functional groups in PLA/HAp 3D scaffolds are not cytotoxic.

Phase transformation study

Figs. 7 and 8 show stacked X-RD results for C1 and C2 respectively. Fig. 7 shows the presence of pure HAp peaks. However, new peaks are apparent due to the presence of PLA. HAp particles have crystalline structures with characteristic sharp diffraction peaks, as seen at $2\theta = 25.9^0$ and 31.9^0. One could note the difference in the intensity of the peaks value in relation to the Ct of HAp within the phase lattice.

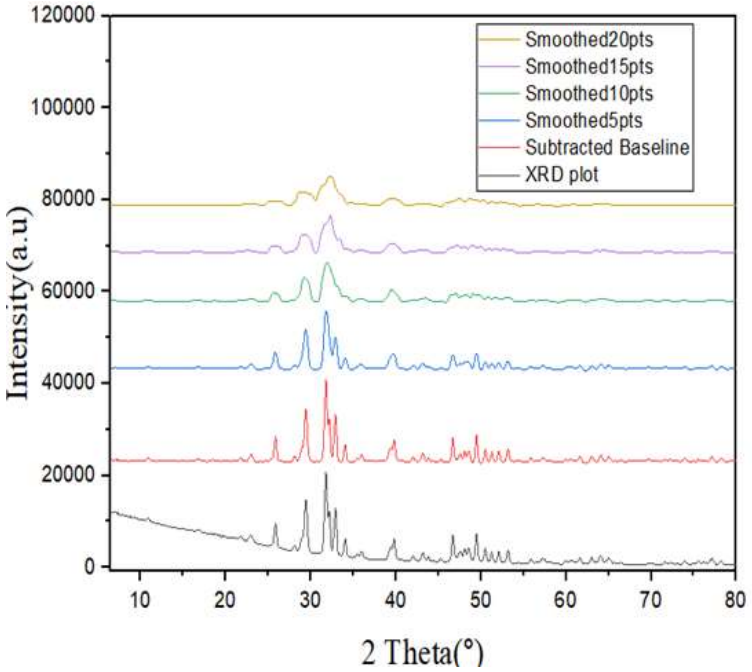

Figure 7: Stacked X-RD spectra for C1.

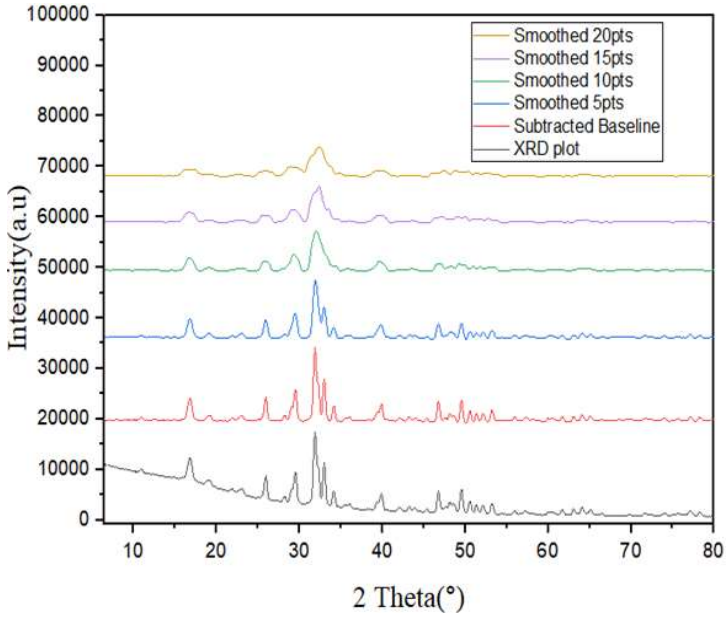

Figure 8: Stacked X-RD spectra for C2.

It is noteworthy that PLA particles have semi-crystalline structures and peaks at 2θ = 16.7 and $19.0^{0.}$ However, no identified characteristic PLA peaks were seen in X-RD patterns for C1, since C2 has a higher Ct of diffused particulates. Nevertheless, it is expected that a sufficient amount could form proper dissolution within the intermetallic phase trend, thereby promoting visible stability. Meanwhile, the intensity of this peak decreased with

increasing Ct from HAp in the 3D scaffold [12-14]. The effect of varying the Ct of HAp in the scaffold was also evident in the samples's crystallinity. C1's crystallinity was 93.61%, as described in Fig. 7, while that of C2 was 90.39%, as seen in Fig. 8.
From all indications, C1 is more crystalline in nature, due to the Ct of HAp present, than 45PLA/55 HAp [13].

Conclusions

In this study, HAp from eggshells was successfully extracted, and PLA/HAP 3D scaffolds were fabricated using sol-gel method. Moreover, SEM shows that 3D PLA/HAp scaffold with the highest Ct of PLA had more consistent crystal formation and weaker grain boundaries. PLA provides mechanical strength, acting as polymeric binding agent in 3D scaffolds. FTIR analysis of 3D scaffolds agreed with PLA's chemical properties. Peaks were present in single and double bond regions. There were no peaks indicating the presence of aromatic structures. Results also confirm that, under X-RD spectra, the presence of PLA and HAp in 3D scaffolds was observed. PLA particles have semi-crystalline structures, while HAp ones are crystalline.

Conflict of interest

The researchers declare that there is no conflict of interest during and after the study.

Abbreviations

C1: 15PLA/85HAP composition
C2: 45PLA/55HAP composition
Ct: concentration
FTIR: Fourier transform infrared spectroscopy
H_3PO_4: phosphoric acid
HAp: hydroxyapatite
PLA: polylactic acid
SEM: scanning electron microscopy
X-RD: X-ray diffraction

Authors' contribution

E. C. Makinde: wrote manuscript. **D. O. Daramola**: inserted tables and figures. **O. S. I. Fayomi**: supervised research.

References

1. Aworinde AK, Taiwo OO, Adeosun SO et al. Biodegradation profiles of chitin, chitosan and titanium reinforced polylactide biocomposites as scaffolds in bone tissue engineering. Arab J Basic Appl Sci. 2021;(28)1:351-359. https://doi.org/10.1080/25765299.2021.1971865
2. Raucci MG, Guarino V, Ambrosio L. Hybrid composite scaffolds prepared by sol-gel method for bone regeneration. Comp Sci Technol. 2010;70(13):1861-1868. https://doi.org/10.1016/j.compscitech.2010.05.030

3. Chandra G, Pandey A. Biodegradable bone implants in orthopedic applications: A review. Biocybern Biomed Eng. 2020;40(2):596-610. https://doi.org/10.1016/j.bbe.2020.02.003
4. Kawu AA, Sha DG, Sough TD. Autologous Bone Grafts Use in Orthopaedic Practice in Abuja. Niger J Orthop Traum. 2009;8(2):1. https://doi.org/10.4314/njotra.v8i2.48301
5. Dimitriou R, Jones E, McGonagle D et al. Bone regeneration: current concepts and future directions. BMC Med. 2011;9(1):1-10. https://doi.org/10.1186/1741-7015-9-66
6. Akter F, Ibanez J. Bone and Cartilage Tissue Engineering. In Tissue Engineering Made Easy. 2016:77-97. Academic Press.
7. Bhaskar B, Owen R, Bahmaee H et al. Composite porous scaffold of PEG/PLA support improved bone matrix deposition in vitro compared to PLA-only scaffolds. J Biomed Mater Res Part A. 2018;106(5):1334-1340. https://doi.org/10.1002/jbm.a.36336
8. Amini AR, Laurencin CT, Nukavarapu SP. Bone Tissue Engineering: Recent Advances and Challenges. Crit Rev Biomed Eng. 2012;40(5):363-408. https://doi.org/10.1615/critrevbiomedeng.v40.i5.10
9. Zhang X, Liu W, Yang D et al. Biomimetic super tough and strong biodegradable polymeric materials with improved thermal properties and excellent UV-blocking performance. Adv Funct Mat. 2019;29(4):1806912. https://doi.org/10.1002/adfm.201806912
10. Weng W, Zhang B, Zhao L et al. Fabrication and properties of PLA/nano-HA composite scaffolds with balanced mechanical properties and biological functions for bone tissue engineering application. Nanotechnol Rev. 2021;10(1):1359-1373. https://doi.org/10.1515/ntrev-2021-0083
11. Nandiyanto A, Oktiani R, Ragaditha R. How to Read and Interpret FTIR Spectroscope of Organic Material. Indon J Sci Technol. 2019;4(1):97-118. https://doi.org/10.17509/ijost.v4i1.15806
12. Athanasoulia I, Christoforidis M, Korres D et al. The effect of hydroxyapatite particles on crystallization and thermomechanical properties of PLLA matrix. Pure Appl Chem. 2017;89(1):125-140. https://doi.org/10.1515/pac-2016-0912
13. Morsi M, Hezma A. Effect of iron doped hydroxyapatite nanoparticles on the structural, morphological, mechanical and magnetic properties of polylactic acid polymer. J Mat Res Technology. 2019;8(2):2098-2106. https://doi.org/10.1016/j.jmrt.2019.01.017
14. Batakliev T, Georgiev V, Kalupgian C. Physico-chemical Characterization of PLA-based Composites Holding Carbon Nanofillers. Appl Compos Mater. 2021;28(4):1175-1192.